Particle Driven Flow down an Incline into a Linear Stratification

Kate Snow
Australian National University

October 1, 2013

1 Introduction

1.1 Motivation

Particle driven gravity currents occur commonly in nature; pyroclastic plumes in the atmospheric setting; turbidity currents in the ocean and the dumping of particle-rich pollutants from industrial means. But the most common form of particle laden currents is that of the turbidity current, sediment laden flows where the sediment suspension is due to the turbulent nature of the flow. These currents occur at the outflow of rivers into the ocean [22, 23], are generated by storm waves impacting the coast [28] and occur in regions of submarine landslides or due to tectonic activity [18]. Turbidity currents are also responsible for the transportation of sediment on a global scale [20], defining the main mechanism that allows sediment to be transported to the deeper ocean [20, 31, 24, 17, 11, 16]. Because of their impacts in global sediment transport, identifying where such currents are dominant and their flow characteristics is an important consideration in understanding the effects of outflowing sediment rich rivers into ocean and their role in erosion and deposition over continental slopes and submarine canyons. Such knowledge is also important in identifying regions of hydrocarbon reservoirs [17, 27], and of paramount importance in consideration of engineering construction and infrastructure near river mouths [22, 23] and on continental shelves [6, 17].

It is not only important to consider where the sediment may be deposited, it is also important to consider at what depth the turbidity current will intrude if it were hyperpycnal, that is, has a density greater than the surface ambient and hence flows below the surface. For example, if a particle pollutant were to intrude at the surface of the ocean, there is important consideration that must be taken into account when considering the effects the pollutant will have on coastal flora and fauna, whereas if the pollutant were to intrude at depth, its removal becomes more difficult and the environmental effects potentially less clear. Risk assessments of a spill therefore would be aided by knowing the intrusion depth of particle laden gravity currents.

A further motivation for knowing the intrusion depth and characteristics of particle laden currents is provided through the work of Clark et al . [8]. In this paper, the extreme cooling event of the Holocene Climate 8.2 kya is investigated, where the believed cause of

the cooling was due to a fresh water flux at the surface of the North Atlantic after the catastrophic drainage of two super lakes. But if this were the case, then why was the constant flux of fresh water occurring prior to the flood over a course of roughly 100 yrs not causing a change in the overturning and hence a similar cooling? Clark et al .[8] argues that the reason there is no change in the overturning prior to the flood is due to the outflowing waters being sufficiently turbid to become particle laden and so descend beneath the surface. To be able to understand such processes more precisely it becomes important to develop an increased understanding of the outflow characteristics and intrusion of a particle laden gravity current.

1.2 Previous Studies

Only limited observational records exist for the occurrence and flow of turbidity currents. This is due to the difficulty in predicting the time and frequency of turbidity currents as well as the destructive nature of such sediment laden currents [32, 26]. Due to the lack of observations, it is increasingly important that properties of turbidity currents are analysed in both the experimental and theoretical fields to allow for an increased understanding of the properties and interactions of such currents.

Many previous studies exist that investigate the nature of turbidity currents, the majority of which only apply to the case where the ambient fluid is of a constant density. Such studies include the numerical study of Hurzeler et al. [15] which considers a flat bottom set-up and experimental and theoretical analyses[12, 13, 4, 30] which again all consider only flat bottom cases.

Cases where the bottom is sloping are considered in, for example Parson et al. [25], where they investigate the production of hyperpycnal plumes on a sloping bottom from the convective instabilities produced from a hypopycnal plume. Bonnecaze et al. [5] also looks at flows of particle laden currents on sloping bottoms. In this case they consider an experimental and theoretical perspective where the current flows into a constant density ambient. The only experimental and theoretical study to consider the effects the of stratification of the ambient fluid for a propagating particle laden current is that of de Rooji [9]. In this study they investigate the settling process, the ambient density and the production of internal waves. However, the set-up is flat bottom and investigates an intrusive current rather than a flow initially propagating along the bottom, such as would occur for hyperpycnal turbidity currents flowing out from rivers and is the main consideration of this report.

1.3 Outline

None of the studies outlined in Section 1.2 include both the effects of slope and stratification as has been performed for studies of saline gravity currents [21, 1, 2, 34, 7]. But to capture the characteristics of a turbidity current flowing into the ocean, both the continental slope and the ocean stratification must be taken into account. This means there is a clear gap within the current studies of turbidity currents and hence a gap in attaining a complete understanding of the features of particle laden, their flow characteristics and their sediment transport properties. Hence, the study reported here provides the initial steps and means to fill the research gap by combining both the effects of slope and ambient stratification in the investigation of particle laden flows. This is done through laboratory experiments, the

set-up of which is outlined in Section 2, and scaling theory presented in Section 3. Results and an example application of the theory are presented in Section 4 and Section 5 with final conclusions in Section 6.

2 Experimental Set-up

Experiments were conducted in a rectangular tank of dimensions, $L = 120.8$ cm, $H = 8.5$ cm and $W = 4.5$ cm . The tank was raised at one end to produce the sloping bottom, where two slope angles were considered, that of $\theta = 8.4^\circ$ and $\theta = 4.4^\circ$, the largest value being the greatest angle possible to allow the entire bottom of the tank to act as a sloping boundary. A Perspex gate edged with foam seal provided the means to produce the lock in which the interstitial fresh water and particle mixture was created. The interstitial fluid density was always that of fresh water (0.998 g cm^{-3}) and the particles were always glass spheres of density 2.5 g cm^{-3}. The diameter of the particles, d, varied between experiments with the particles taking five possible values of 1-38 μm, 13-45 μm, 38-53 μm, 53-75 μm and 63-90 μm. In addition, a few salt solution gravity currents were considered, in which case no particles are used, rather the salt solutions experiments provided a base case to compare the particle currents to.

The ambient fluid was created using the double bucket method of producing a linear stratification. To take into account the slope at the bottom of the tank however, the method was modified so that the salty bucket contains half the volume of the fresh water bucket, the density of the flow out of the salt water bucket changes quadratically in time, and thus the stratification in the triangular domain changes linearly with depth. The stratification values used were approximately $N = 0$, 1.12, 1.9 and 3.0 s^{-1} where N is the buoyancy frequency and the stratification was measured after the tank was filled using six densitometer measurements taken evenly with height at the deepest end of the tank. Figure 1 provides a summary of the key characteristics of the experimental set-up.

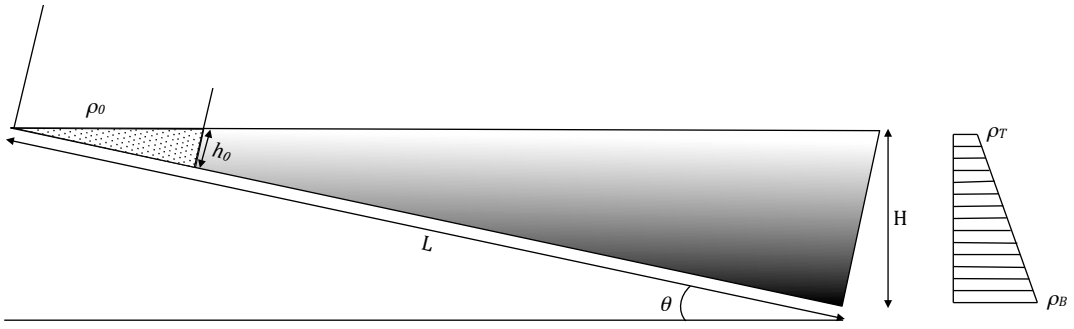

Figure 1: Summary of the experimental setup used in this study.

The height of the lock, h_0, which defines the downslope velocity speed, was varied by changing the position of the lock along the slope so that it may be in deeper or shallower water. The lock heights considered are 3, 4.5 and 6 cm. The density of the particle laden fluid within the lock, ρ_0, was then determined by the mass of particles added to the given volume of fresh water within the lock, with the final lock densities ranging from 1.02 g

cm^{-3} to 1.21 g cm^{-3}. Coloured dye was added to the lock fluid, and after vigorous mixing to ensure the particles are uniformly distributed, the lock was pulled and the flow of the current recorded using a digital camera. Image analysis techniques of the footage of the flow and the progression of the front allows for both down speed velocities and intrusion depth are determined. The intrusion depth here is defined as the point at which the current front first lifts up off the slope and is quantified by the depth z at which this occurs. This depth and the progression of the flow down the slope is indicated in Figure 2.

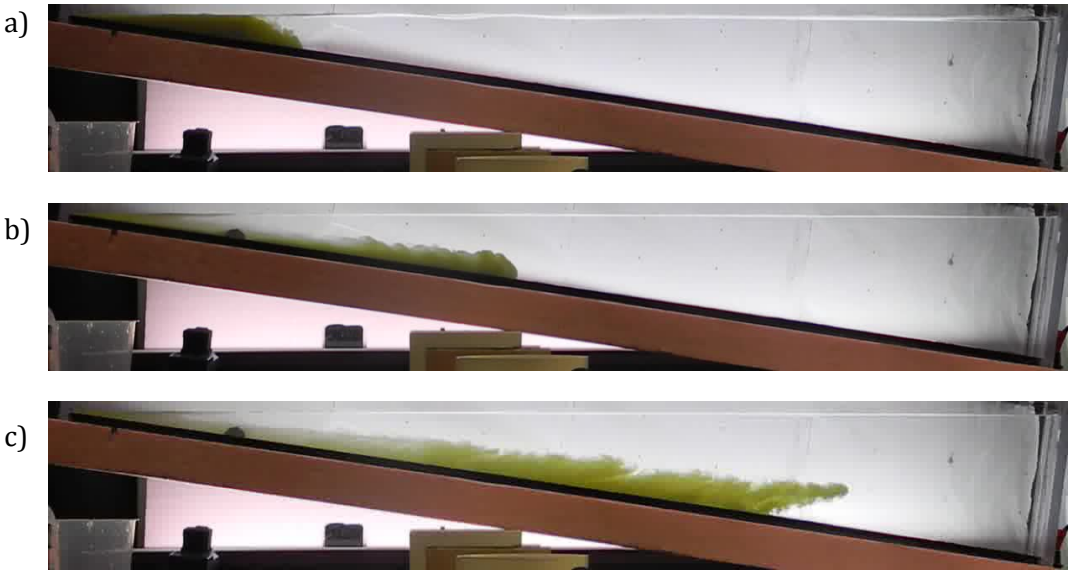

Figure 2: Illustration of the progression of the current a) after the lock is pulled, b) as it flows down the slope and c) after the points of intrusion z, where in this case $N = 1.1$ s^{-1}, $h_0 = 3.3$ cm, $\rho_0 = 1.02$ g cm^{-3} and $d = 1 - 38$ μm.

3 Scaling Theory

Scaling theory is applied to the situation defined in the experimental set-up to produce a theoretical expression for the intrusion depth of a particle laden current. Firstly, consider a particle laden gravity current made up particles of density ρ_P and an interstitial fluid density, ρ_i, flowing down a slope, S, into an ambient fluid that has a constant stratification, N. Then since N is constant, it may be defined by the bottom density, ρ_B, and the density at the top of the tank, ρ_T:

$$N^2 = \frac{g}{\rho_{00}} \frac{d\rho}{dz} = g \frac{\rho_B - \rho_T}{\rho_T H}, \tag{1}$$

where H is the height of the fluid at the deepest end of the tank, g is the gravitational constant, and we have chosen the reference density, ρ_{00} to be ρ_T as we apply the Boussinesq approximation.

With the addition of the slope into the system, the driving force can no longer be assumed to be only buoyancy and inertial forces; now both entrainment and bottom friction need to be considered. However, the effects of friction may be ignored if the Reynolds number is high and hence the flow is within the turbulent regime. The Reynolds number is given by:

$$Re = \frac{Uh_0}{\nu} \tag{2}$$

where ν is the kinematic viscosity of the fluid (for fresh water ν 10^{-6}), U is the speed of the current ($0.05 - 0.1$ m/s for the majority of the flow before the intrusion depth is reached), h_c is the height of the current (0.03 at the head) and θ is the angle of the slope ($4 - 8°$). Hence, given the approximate values for each term, it is verified that for all cases the Reynolds number for the flow is of the order of 1500-3000 meaning the flow is always within the turbulent regime and the effects of friction may be ignored.

3.1 Flow Separation

In a uniformly stratified fluid, the velocity of the gravity current at the front is dependent on the stratification:

$$U = F_N N h_0 \tag{3}$$

where F_N is the Froude number for stratified ambients and expected to be of the order of 0.266 [19] to 0.25 [33].

For a uniform ambient however, we expect the constant front velocity to depend on the reduced gravity, taking the form:

$$U = F_0 \sqrt{g' h_0} \tag{4}$$

where now the Froude number, F_0 for a constant density ambient is of order 0.5 based on theory [3], but is often closer to 0.48 in experiments [29]. We have assumed that the slope is small so that the the effects of the slope on the front velocity may be ignored, an assumption that is verified by [7] where they show that there is little dependence on the front velocity with slope. Hence, assuming that the initial flow is large enough that viscous forces are unimportant (as expected for the high Reynolds number situation considered here) and the size of the lock is unseen by the flow in the initial stages, the initial front velocity U may be defined in terms of the $\beta = \frac{Nh_0}{\sqrt{g' h_0}}$:

$$U = \sqrt{g' h_0} f(\beta) \tag{5}$$

where g'_0 is the initial reduced gravity and f is a function representing the change in the Froude number when going from uniform ambient to a uniformly stratified fluid, i.e. $f(0)$ approaches 0.5 and decreases to 0.25 when $Nh_0 = \sqrt{g' h_0}$, i.e. $f(1) = 0.25$. The trend of f is found experimentally and given in Figure 7. After initial experimental results (refer to Section 4.1), it is found that the majority of the flow before the intrusion depth is reached occurs at a constant velocity. Therefore, to a first approximation, we are going to assume that U is constant.

3.1.1 Dilution of Interstitial Fluid

In order to determine the intrusion depth, all the factors that effect the density of the current with time must be considered. The key characteristics of particle laden currents that change the overall density are; the entrainment of the interstitial fluid with the ambient fluid, and the settling of the particles as the current progresses down the slope. Firstly considering the entrainment of the interstitial fluid, we assume that it occurs independently of the particles settling out.

Due to the thinness of the tank, there is assumed to be no cross-slope velocity and effectively the flow is represented as a 2D flow. A box model set-up is then applied to the interstitial fluid flow as shown in Figure 3, where h_c is the height of the current, l_c is the front position down the slope, $V = h_c l_c$ is the volume of the interstitial and ρ_a is the ambient density. The vertical coordinate is taken to be perpendicular to the slope and defined as h and the horizontal co-ordinate is taken perpendicular to the slope, defined as l.

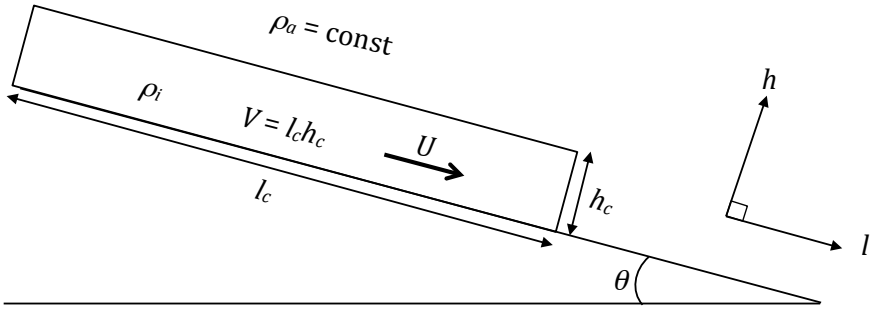

Figure 3: Summary of the box model set-up for the interstitial fluid flow down the slope.

The entrainment is assumed to be a function of the speed of the flow and an entrainment coefficient defined here as $E = 0.08$ and taken to be constant. The change in volume of the 2D current may then be written as:

$$\frac{dV}{dt} = U_e l \tag{6}$$

where U is the front velocity, $U_e = EU$ is the entrainment velocity, and dt is the change in time. Since the velocity of the current may be assumed constant from section 3.1 and the entrainment coefficient is constant, the change in volume may be defined from (6) as:

$$dV = EU(l_0 + Ut)dt \tag{7}$$

where $l_c = l_0 + Ut$. Hence, the change in density of the interstitial $d\rho_i$ is given through the change in volume dV by:

$$\rho_i + d\rho_i = \frac{\rho_i V_0 + \rho_a EU(l_0 + Ut)dt}{V_0 + EU(l_0 + Ut)dt} \tag{8}$$

where l_0 is the initial lock length, V_0 is the initial lock volume and ρ_a is the density of the ambient. The Boussinesq approximation is applied for the ambient density allowing ρ_a to

be a constant. Such an approach is necessary to avoid numerical solutions for this simple scaling theory approach.

Since dt is small, the denominator of (8) can be expanded through a Taylor series leading to, at the first order approximation:

$$d\rho_i = (\rho_a - \rho_i)\left(\frac{EUl_0}{V_0} + \frac{EU^2}{V_0}t\right)dt = \frac{(\rho_a - \rho_i)}{V_0}dV \tag{9}$$

which is integrated to give:

$$\rho_i = \rho_a - (\rho_a - \rho_{i0})e^{-\frac{V}{V_0}+1} \tag{10}$$

where ρ_{i0} is the initial density of the interstitial fluid, i.e. the density of fresh water. Hence, an equation representing the change in density of the interstitial fluid due to entrainment is given.

3.1.2 Particle Settling

The second effect that must be considered for the change in density of the particle laden current is the settling of the particles. The particles being used in this experiment are that of glass spheres and are assumed to not flocculate within the current. Suitably low concentrations of the particles are also used (volume fractions < 0.15) so it is assumed that there is no hindrance to settling of the particles as they travel with the current. It is further assumed that the flow is sufficiently turbulent that the particles are uniformly mixed through the current, yet none are lost through the top. This is the most common approach to defining the sedimentation process [14, 4]. Hence, to a first approximation, the change in concentration of the particles within the current is defined through the Stokes settling velocity, U_s, acting at the lower boundary of the current. Though the particles may vary in size in a particular experiment through a small range (e.g. d = 38-53 μm), the variation of U_s is considered negligible and a constant settling velocity is taken for a single particle type.

The Stokes settling U_s defining the speed at which the particles settle out of the interstitial fluid is given by:

$$U_s = \frac{gd^2(\rho_P - \rho_i)}{18\mu} \tag{11}$$

where μ is the dynamic viscosity ($\mu = 1 * 10^{-6}$Pas for fresh water) and d is the diameter of the particles. Hence, the change in mass of the particles dm_p within the current is given by:

$$dm_p = -\frac{m_p}{h_c}U_s dt = -\frac{m_p l_c U_s}{V}dt \tag{12}$$

Dividing both sides of (12) by (7) gives an equation in terms of V and m_p which when integrated yields:

$$m_p = m_{p0}\left(\frac{V}{V_0} - 1\right)^{-\gamma} \tag{13}$$

where $\gamma = \frac{U_s}{U_e}$, is the ratio of the settling velocity to the entrainment velocity.

Applying a change of variables so that (13) may be written in terms of the volumes fraction of particles, ϕ, where $m_p = \rho_P V \phi$ gives:

$$\phi = \phi_0 \left(\frac{V}{V_0} - 1 \right)^{-\gamma - 1} \tag{14}$$

Hence, we now too have an equation defining the change in the volume fraction of the particles with time. Combing this with the change in the density of the interstitial fluid will then provide the overall change in density of the particle laden current.

3.1.3 Separation Depth

With both the effects of entrainment and particle settling accounted for, the depth of the intrusion or separation of the fluid may be defined. This occurs when the density of the current ρ_c equals the density of the ambient along the slope ρ_s, where ρ_s is a function of position due to the linear stratification of the ambient. Hence, solving for $\rho_c = \rho_s$ where $\rho_c = \rho_i + \phi(\rho_P - \rho_i)$ gives:

$$\rho_a + (\rho_{i0} - \rho_a) e^{-\frac{V}{V_0} + 1} + \phi_0 \left(\frac{V}{V_0} - 1 \right)^{-\gamma - 1} \left(\rho_P - \rho_a - (\rho_{i0} - \rho_a) e^{-\frac{V}{V_0} + 1} \right)$$

$$= (\rho_B - \rho_T) \frac{l_0 + Ut}{L} + \rho_T$$

Substituting for V and again applying the Boussinesq approximation, assume that $\rho_{i0} = \rho_a = \rho_T$ giving:

$$\phi_0 \left(\frac{V}{V_0} + 1 \right)^{-\gamma - 1} (\rho_P - \rho_T) = (\rho_B - \rho_T) \frac{l_0 + Ut}{L} \tag{15}$$

which can be written as:

$$\phi_0 \left(1 + \frac{EU}{l_0^2 S} (t l_0 + t^2 U/2) \right)^{-\gamma - 1} (\rho_P - \rho_T) = (\rho_B - \rho_T) \frac{l_0 + Ut}{L} \tag{16}$$

where S is the slope. Equation (16) may be solved implicitly in time to determine the points of intrusion, or limits in time may be taken.

3.2 Asymptotic Limits

3.2.1 Time limit $t >> \frac{l_0}{U}$

The first limit to consider is the case where the current flows further than one lock length, that is $t >> \frac{l_0}{U}$. Then $\frac{t^2 U}{2} >> t l_0$ and in (16):

$$t l_0 + \frac{t^2 U}{2} \approx \frac{t^2 U}{2} \tag{17}$$

With this limit, the remaining time dependence is given by $1 + \frac{U_e}{V_0} \frac{t^2 U}{2}$ which may be further simplified.

Case 1. If $\frac{U_e}{V_0}\frac{t^2U}{2} >> 1$ then it is necessary that $t^2 >> \frac{2V_0}{EU^2} = \frac{l_0^2 h_0}{EU^2 l_0} = \frac{l_0^2}{U^2}\frac{S}{E}$ which implies $t >> \frac{l_0}{U}\sqrt{\frac{S}{E}}$. But it has already been noted in this case that $t >> \frac{l_0}{U}$, so this limit simply requires $\sqrt{\frac{S}{E}}$ isn't much less than 1. Considering we expect $E < 0.1$, then we are left with the same limit for anything but slopes that approach 0. Hence, in this limit (16) becomes:

$$\phi_0 \left(\frac{EU^2}{2V_0}\right)^{-\gamma-1} t^{-2\gamma-2} = \frac{(\rho_B - \rho_T)}{(\rho_P - \rho_T)}\frac{Ut}{L} \tag{18}$$

which may be written as:

$$\frac{t}{\tau} = \left(\frac{N^2 \rho_T \sin(\theta)}{g\phi_0(\rho_P - \rho_T)}\sqrt{\frac{2V_0}{E}}\right)^{\frac{-1}{2\gamma+3}} \tag{19}$$

where $\tau = \sqrt{\frac{2V_0}{EU^2}}$. Putting (19) in terms of the intrusion depth z where $z = l_c/\sin(\theta)$ and $l_c = l_0 + Ut$ at the point of intrusion gives the final result:

$$\frac{z}{h_0} = \left(\frac{g_0'}{N^2 h_0}\right)^{\left(\frac{1}{2\gamma+3}\right)} \left(\frac{S}{E}\right)^{\left(\frac{\gamma+1}{2\gamma+3}\right)} \tag{20}$$

where g_0' is the initial reduced gravity. It is seen from (20) that the defining parameter of the system is γ, the ratio of the settling and entrainment velocities.

Case 2. The second option in the limit $t >> \frac{l_0}{U}$ is that $t << \frac{l_0}{U}\sqrt{\frac{S}{E}}$ in which case (16) may be written as:

$$\phi_0 \,(1)^{-\gamma-1} \,(\rho_P - \rho_T) = (\rho_B - \rho_T)\frac{l_0 + Ut}{L} \tag{21}$$

rearranged gives the result:

$$\frac{l}{L} = \frac{\phi_0(\rho_P - \rho_T)}{\rho_B - \rho_T} \tag{22}$$

and substituting for z and $L\sin(\theta) = H$ gives:

$$\frac{z}{H} = \frac{\phi_0(\rho_P - \rho_T)}{\rho_B - \rho_T} \tag{23}$$

which may be written as:

$$\frac{z}{h_0} = \frac{g_0'}{N^2 h_0} \tag{24}$$

The result of (24) shows no dependence on the γ parameter and hence, the entrainment or settling velocity. So effectively, (24) represents the case where the flow travels such a short distance or there is such minimal settling over the period before intruding that these effects have minimal impact on the density of the current before it intrudes.

3.2.2 Time limit $t << \frac{l_0}{U}$

Now consider the opposite case to the previous section, i.e. $t << \frac{l_0}{U}$, the current intrudes less than one lock length along the slope. Then it is clear that $tl_0 + \frac{t^2U}{2} \approx tl_0$ and we must now consider how the term $1 + \frac{U_e}{V_0}tl_0$ evolves with time.

Case 3. First take $t << \frac{V_0}{U_e l_0} = \frac{l_0}{U}\frac{S}{E}$, which is true for anything but where the entrainment approaches zero. In these experiments the entrainment parameter E is found to be approximately 0.08 and the slope ranges from 0.07 to 0.15, hence this limit is valid for all the experiments performed here that intrude at less than one lock length. The result of applying these limits then provides the same results as was found in Case 2 for equation (24).

Case 4. In this case $t << \frac{l_0}{U}$, but assume now that the slope approaches zero so that $t >> \frac{l_0}{U}\frac{S}{E}$. Then from (16) this gives:

$$\phi_0 \left(\frac{U_e}{h_0}t\right)^{-\gamma-1} (\rho_P - \rho_T) = (\rho_B - \rho_T)\frac{l_0}{L} \tag{25}$$

which can be written as:

$$\frac{Ut}{h_0} = E\left(\frac{g_0'}{N^2 h_0}\right)^{\frac{1}{\gamma+1}} \tag{26}$$

Writing (26) in terms of z gives the intrusion depth as:

$$\frac{z}{h_0} = ES\left(\frac{g_0'}{N^2 h_0}\right)^{\frac{1}{\gamma+1}} \tag{27}$$

again providing the dependence of the intrusion depth to the parameter γ.

3.3 Particle Concentration at Intrusion

It is often useful to provide an indication of the quantity of particles that have settled out along the slope and the amount that continue to be transported with the intruded fluid. This provides an indication of where the particles will end up and at what depth. The amount of particles remaining within the intrusion can then be determined by knowing the density of the interstitial fluid at the point of intrusion and the total current density at intrusion. Both of these can be found by knowing the intrusion point z. The interstitial density (10) in terms of the intrusion depth z is given by:

$$\rho_i = \rho_a - (\rho_a - \rho_{i0})e^{-\frac{E}{S}\frac{z^2}{h_0^2}} \tag{28}$$

where:

$$\rho_a = \frac{\rho_s(z) + \rho_T}{2} = \frac{N^2\rho_T z}{2g} \tag{29}$$

is the mean density of the ambient fluid over the depth of intrusion z. Hence, solving $\rho_c = \rho_i + \phi(\rho_P - \rho_i)$ for ϕ will provide the volume fraction of particles at the point of intrusion, ϕ_i, and is found to be represented by:

$$\phi_i = \frac{\frac{N^2\rho_{00}z}{g} + \rho_T - \rho_{i0} + (\rho_a - \rho_{i0})\, e^{-\frac{E}{S}\frac{z^2}{h_0^2}}}{\rho_P - \rho_a + (\rho_a - \rho_{i0})\, e^{-\frac{E}{S}\frac{z^2}{h_0^2}}} \tag{30}$$

Applying the Boussinesq approximation so that $\rho_T = \rho_{i0} = \rho_a$ then gives:

$$\phi_i = \frac{h_0 N^2 \frac{z}{h_0}}{g\left(\frac{\rho_P}{\rho_{i0}} - 1\right)} \tag{31}$$

Hence, (31) provides an indication of the amount of particles deposited down the slope and the amount continuing to intrude into the ambient fluid. If we also assume that there is no entrainment after the current intrudes and the only change in density of the current is due to the settling of the particles, then the settling of the particles over time may be defined through:

$$\phi = \phi_i e^{-\frac{U_s}{h_c}t} \tag{32}$$

This leads to a representation of where the particles will end up over the entire course of the current flow and settling process.

3.4 Fingering

One dominant feature of the flow is the presence of smaller intrusions or fingers prior to the current reaching the final intrusion depth. These fingers are seen also in the saline solution gravity currents and have been noted previously as a double outflow effect [2] and a similar effect is found when a time varying density enters a continuous stratification [10]. This fingering is illustrated in Figures 4 and 5:

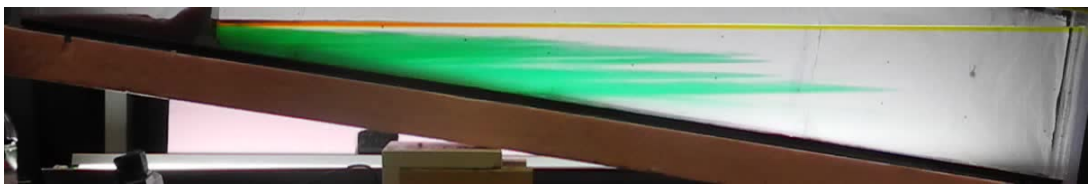

Figure 4: Fingering intrusion observed for $N = 1.9$, $\rho_0 = 1.2$, $\theta = 8.4$, $d = 13 - 45$ μm and $h_0 = 3$ cm (green dye). Note: the red and yellow dye are previous lock exchange experiments run in the same tank set-up, but have not affected the overall startification of the ambient and so do not affect the results presented here.

The only difference in the runs of Figures 4 and 5 is the height of the lock used, and therefore, the speed of the current. In Figure 5, the current speed is greater than that of Figure 4 and it is also noted that the average spacing between fingers appears to be larger. Hence, it would appear, to first order, that the fingering spacing is a result of the degree of stratification N and the speed of the current as it flows down the slope U. Dimensional analysis therefore would indicate that the spacing of the fingers is of the order of U/N.

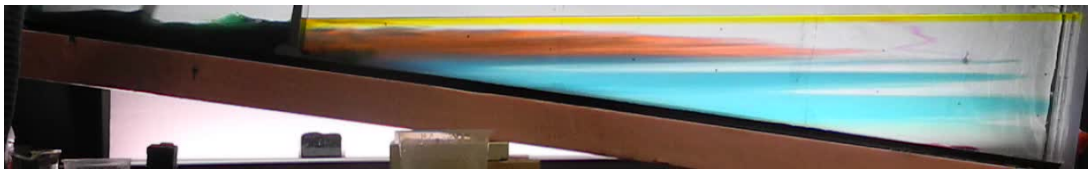

Figure 5: Fingering intrusion observed for $N = 1.9$, $\rho_0 = 1.2$, $\theta = 8.4$, $d = 13 - 45$ μm and $h_0 = 6$ cm (blue dye). Note: the red and yellow dye are previous lock exchange experiments run in the same tank set-up, but have not affected the overall startification of the ambient and so do not affect the results presented here.

4 Results

4.1 Front Velocity

The experimental studies provide a clear observation of the flow processes and characteristics. After the gate is released, the gravity current front is quickly set-up and flows down the slope until it either hits the end of the tank or reaches the point of intrusion. As it flows, the turbulent nature of the current is clear and entrainment occurs at the upper edge boundary and head of the current. Once the current intrudes, if it is still heavily laden with particles, some further particle settling is observed to occur.

Measurements of the front position as it travels down the slope are taken against time using image analysis tools in Matlab. An example of such results are shown in Figure 6 where the position of currents of density 1.02, 1.1 and 1.2 g cm^{-1} are given. It is seen from Figure 6, that a constant slope of position versus time is maintained from the initial set-up of the current nearly all the way to the intrusion point where the slope position becomes a maximum. This constant slope gives the speed of the current front as it travels.

It may also be noted that there are some oscillations of the position on the slope after the first intrusion in Figure 6. These oscillations are due to the effects of rebounding internal waves off the back wall to the tank, however such internal waves initiated by the flow do not affect the current until after the intrusion point has been reached and so are ignored in this study.

With the front velocities measured for each case, the dependence of the velocity to the stratification can be determined as explained in Section 3.1 and (5) and the results of front velocity for changing stratification is shown in Figure 7. It can be seen from Figure 7, that for zero stratification, the non-dimensional front velocity approaches a value of 0.5, that is, the expected value of Froude number for a constant density ambient. As the stratification increases however, the non-dimensional frontal velocity decreases until the point at which $Nh_0 = \sqrt{g_0' h_0}$ and $\beta = 1$ where the non dimensional frontal velocity is approaching 0.25. This is again the approximate value expected for this case and so further verifies the trend provided in Figure 7 indicating the effects of increasing stratification to front velocity.

4.2 Intrusion Depth

The depth of intrusion z is determined as the depth at which the head first lifts up off the slope, meaning experimentally it is measured as the maximum position of the front along the

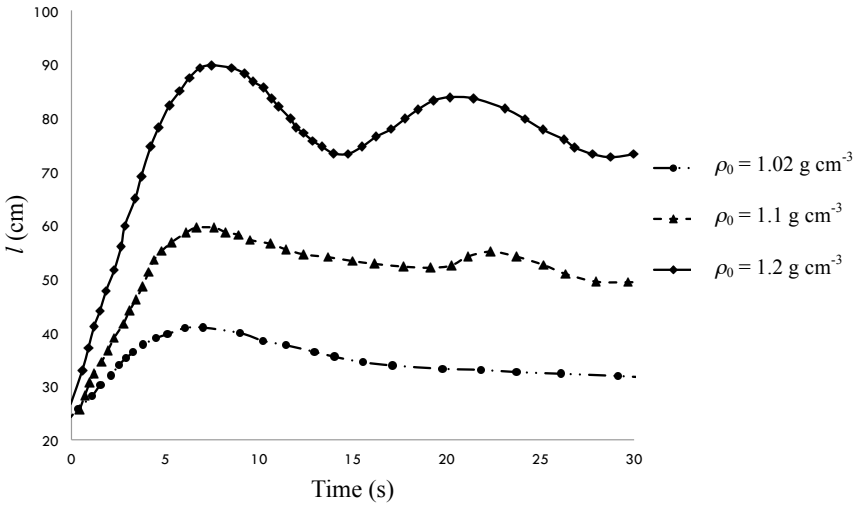

Figure 6: Slope position of gravity current front for $\rho_0 = 1.02$, 1.1 and 1.2 g cm^{-1}, $d = 13-45$ μm, $\theta = 8.4°$, $N = 3.0$ s^{-1} and $h_0 = 3$ cm.

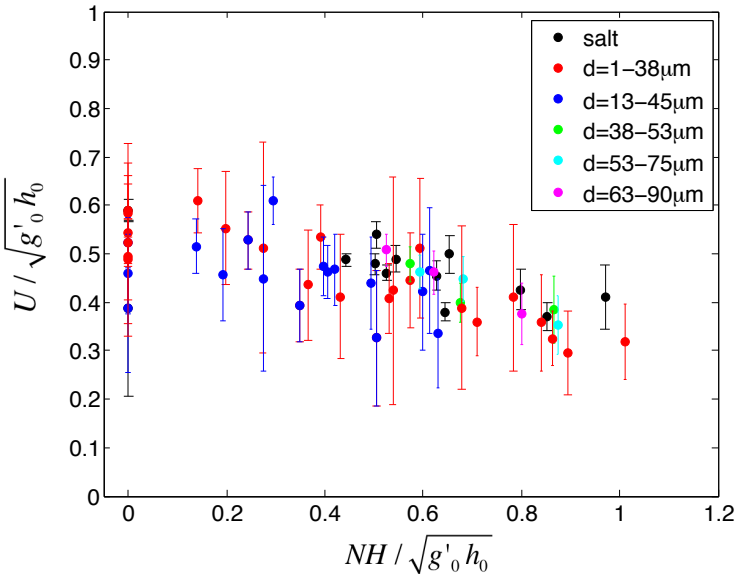

Figure 7: Non-dimensionalized front velocity U versus the ratio of the effects of stratification N and initial buoyancy determined from the reduced gravity g_0'.

slope as may be observed in Figure 6. The measured z/h_0 values are then plotted against the theoretical value of z/h_0 given by case 1, (20), for currents that intrude less than one lock length down the slope and case 3, (24), for currents that travel more than one lock length and the results presented in Figure 8.

It is seen from Figure 8a) that values for z/h_0 less than one do not fit the theoretical results well. This is to be expected as the theory in this case is within the time limit where

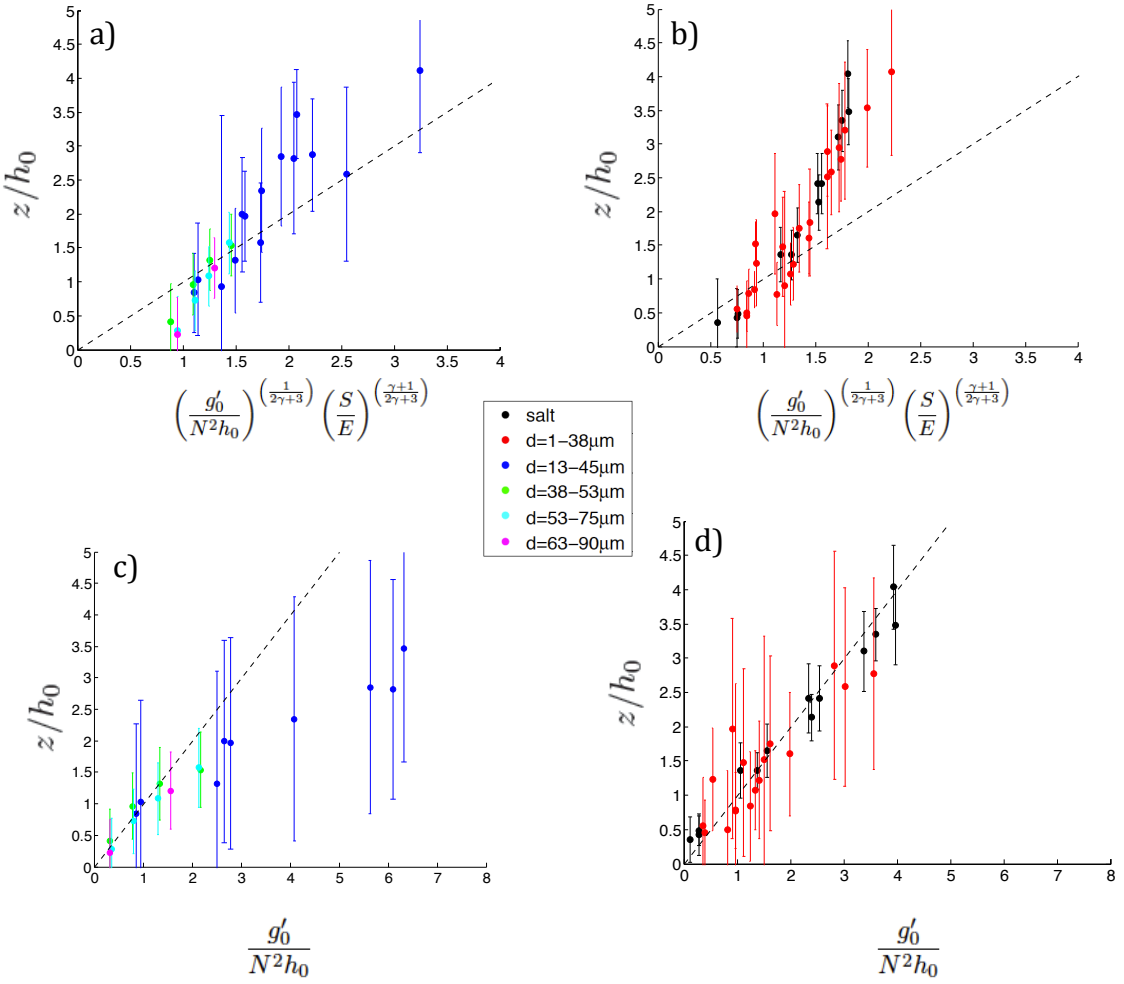

Figure 8: Non-dimensional intrusion depth versus theoretical intrusion depth for currents that intrude greater than one lock length a) and b) and less than one lock length c) and d), where a) and c) show the larger particles intrusions and b) and d) only the smallest particle and salt solution intrusions.

the current is assumed to flow more than one lock length. Yet there is good agreement in Figure 8a) for currents travelling greater than one lock length for these larger particle cases, verifying the theory. However, for Figure 8b), the same agreement is not seen between the theory and the smallest particle size and the salt solution experiments. Yet it is noted that, despite the theory being within the less than one lock length limit for Figure 8d), all the experiments, whether travelling less than or more than one lock length, match the theoretical prediction in this case. What this indicates is that essentially, the dependence of these flows on the γ parameter is not present and so the dependence of the flow on the settling velocity to entrainment velocity is absent. This is expected for the saline solution as in that case, with no particles, $\gamma = 0$, and for the smallest particle cases where $d = 1 - 38$ μm, the settling velocity is so small that it does not play a dominant role in affecting the

intrusion depth of the flow. If a longer tank had been used and the flow permitted to travel over a longer distance then potentially the effect of settling would play a more dominant role for the smallest particle currents, but over the short distances allowed, the settling was too slow to have a large impact on the density of the current.

There is close match between experiments and theory when z/h_0 is less than one in Figure 8c) where the theory is within the less than one lock length limit, again verifying the theory for the larger particle currents. It is also noted from Figure 8c), that the further from the one lock length limit the current has intruded, the further the deviation of the experimental results to the theory. This indicates the necessity of having both the case 1 and case 3 theories in defining the characteristics of the flow for the larger particles cases and hence, the importance of the γ parameter in defining particle laden currents where the particles play a dominant role.

4.3 Intrusion Fingers

One dominant characteristics of the particle current is the presence of intrusion fingers. Comparing the saline current fingers to that of the particle laden currents, it is noted that the fingering appears to be more distinct in the particle currents. This is potentially due to the shallower tail region of the flow which leads to increased settling as indicated from (12) for a smaller value of h_c. Hence, some fluid intrudes at shallower depths than would occur in a saline current, leading to a clearer and wider range of fingering.

Applying the scaling analysis of Section 3.4, the theoretical values of U/N is plot against the mean measured finger spacing z_f, where z_f is determined with the application of Matlab image analysis tools. The results of z_f versus U/N are shown in Figure 9.

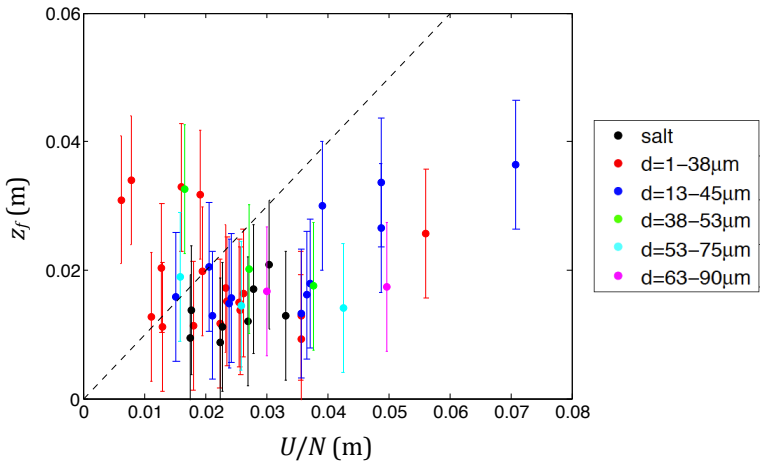

Figure 9: Mean measured distance between fingers z_f versus U/N.

From Figure 9, no clear trend is seen in the data given. It is also possible that not all the fingers being produced were fully discernible due to the spreading width of the fingers, two fingers may have merged and so the simple method of searching the image for finger positions may not have been robust enough to capture the full fingering effects. Such fingering however, could potentially impact the transport and outflow properties of particle

laden plumes as they travel down a slope into a stratified fluid and so would be of benefit to investigate further.

5 Application

The study of Clark et al. [8], uses shallow water equations solved numerically to provide an indication of the properties of the outflowing water entering the North Atlantic prior to the 8.2 kya extreme cooling event. The main limitation of their model however, was that they did not have a suitable indication of the concentration of particles required to cause the water to sink below the surface. The only condition at hand was that of a threshold value for hyperpycnal plumes, that is, calculating the fraction of particles required so that the density of the outflowing water is greater than the density of the ambient. Under this assumption, it means that there must be a volume fraction of particles of 0.0206. Clark et al. [8] also note that under such conditions, the particle levels are quite large but not impossibly high for glacial meltwaters.

A comparison between the value of Clark et al. [8] and a value determined from the theoretical analysis presented in this study could provide an indication of a more suitable condition for the outflowing meltwaters to become hyperpycnal and flow below the surface. Such knowledge will provide an increased understanding of the properties of the outflowing water and the events prior to the extreme event of the Holocene Climate 8.2 kya. To apply the theory presented here, relevant parameters must be chosen to determine the volume fraction of particles needed for the intrusion to sink below the surface. In particular, rather than simply looking at what densities would be required to allow the current to sink just below the surface where it is highly likely that some surface fresh-water fluxes would indeed occur, rather it is more relevant to determine values of particles fractions that would mean no fresh water flux reached the surface even some time after the intrusion. Hence, consider the case where the outflowing water intrudes below the thermocline where the stratification of the overlaying waters would inhibit the rise of any remaining fresh water. Further, if the water did intrude to depths of say 100 m, the approximate thermocline depth, then the entrainment that occurs as it descends would remove the majority of the fresh water from the North Atlantic. Hence, taking $z = 100$ m, we also then define the density of the ambient as that of salt water $\rho_a = 1.035$ g cm^{-3}, the density of the particles is $\rho_P = 2.700$ g cm^{-3}, [8] and the interstitial density is taken as $\rho_{i0} = 1.00$ g cm^{-3}, that of cold fresh water. The slope then is taken as a typical shallow ocean shelf slope, $S = 0.01$, and the height of the lock is assumed to be $h_0 = 40$ m based on an approximate value from the outflowing river height in Clark et al. [8]. Finally, the entrainment parameter is kept fixed at 0.08 and the stratification is taken as a mean value for the pycnocline range $N = 0.001$ s^{-1}. From these values, the volume fraction of particles required to cause the flow to intrude to 100 m may be calculated, taking a range of particles sizes, $d = 2, 5, 20, 50$ μm, which are the diameters of fine clay, clay, silt and sand respectively, the main sediment expected to be picked up by the flow.

In all cases of particles sizes, the volume fraction of particles required for the outflowing water to sink below 100 m is of the order of 0.0209. This is only slightly larger than that predicted by Clark et al. [8] using the simple threshold method, however it provides a more robust indication of the particle concentrations required to allow the flow to intrude at

depth. Hence, the results here potentially allow for a more complete picture of the nature of the outflowing waters prior to the extreme event and also provides a reasonable value compared to possible particle concentration levels for glacial metlwaters.

5.1 Convective Instabilities

A further note of Clark et al. [8] is that potentially a hyperpycnal plume can be produced at much lower sediment concentration [25]. Parso et al. [25] looks at the development of a hyperpycnal plume from the convective instability produced from a hypopycnal plume as the particles settle out. In their study however, their experimental set-up considered only the case of a constant density ambient, and while the production of a hyperpycnal plume from a hypopycnal plume was also observed in the constant ambient experiments of this report, (refer to Figure 10) the continued settling of particles later led to the interstitial fluid of the hyperpycnal plume to become negatively buoyant and return to the surface as shown seen in Figure 10e) meaning for the case of Clark et al. [8], the fresh water flux may still have occurred at the surface. Further, such convective instabilities were not observed in any of the cases where the ambient was stratified. Figure 11 shows the settling of particles after the intrusion occurs within a lineally stratified ambient. It is observed that the particles separate from the flow and settle at a rate proportional to the settling velocity with no convective instabilities developed. It seems then that the presence of the stratification hinders the production of the convective instabilities and so prevents any further descent of the interstitial fluid. Hence, when considering an intrusion into the ocean where stratification plays an important role, in order to maintain the fresh water flux intruding at depth and not returning to the surface, particle concentrations must be of the order such that the plume is initially hyperpycnal and intrudes at depth.

6 Conclusion

In this study, laboratory experiments were undertaken to investigate the effects of both slope and stratification on particle-driven gravity currents. The slope velocity, intrusion depth and the effects of fingering were all measured. As with studies on saline gravity currents, an initial constant velocity is set-up that may be defined through the initial reduced gravity of the flow and the stratification through the Froude number. The effects of the variation of the front velocity and Froude number to increasing stratification is presented and provides an indication of the dependence of the front velocity to the effect of stratification.

The stratification of the ambient is also found to lead to a fingering effect with multiple intrusions occurring along the slope. This effect has been observed previously only as double intrusion of a saline gravity current [1] and in changing density currents entering a stratified fluid [10]. Quantifying this effect however, has proven to be more difficult than expected. The dependence of the distance between fingers on the front velocity is presented leading to a clear scaling term of U/N, however experiments were unable to verify this results, potentially due to the method of analysis used to calculate the distance between fingers, as some fingers may merge and so not be picked up.

The intrusion depth of the flow is represented through theoretical scaling analysis equations incorporating all the key effects of the flow, in particular that of of the entrainment of

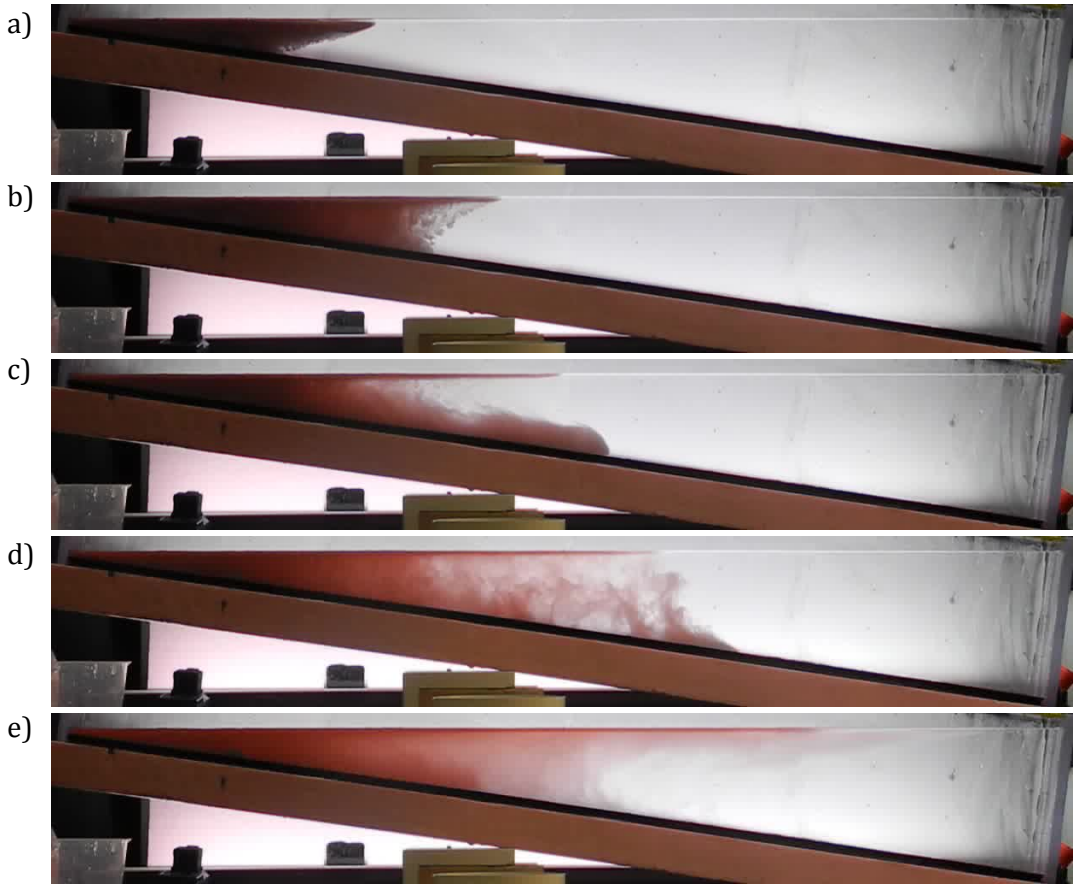

Figure 10: Flow of a particle laden current in a stratified ambient $N = 3.0$ s^{-1}, $\rho_0 = 1.12$ g cm^{-3} with interstitial fluid density 0.998 g cm^{-3}, $d = 13 - 45$ μm and $h_0 = 3$ cm where a) the initial hypopcyanl plume is shown. Instabilities develop b) that lead to the production of a hyperpycnal plume c) which after further settling of particles within the hyperpycnal plume leads to the reversing buoyancy of the interstitial d) and the fluid returning to the surface e) as hypopycnal.

the interstitial fluid and the settling of the particles. These theoretical results are verified by the application of experimental results performed with varying particle sizes, stratifications and particle volume fractions. From these results it is found that one of the key parameters defining the flow is the γ parameter, defining the ratio of settling velocity to entrainment velocity. This parameter becomes increasingly important for larger particles where the settling velocity is greater, while for decreasing particle size, where the current approaches a nature more comparable to that of a dense salt solution, the dependence on this term is no longer present. In the saline and small particle gravity currents, it is instead found that the intrusion depth of the flow may be represented by a simple scaling term dependent on the initial buoyancy of the flow, the lock height and the stratification of the ambient.

With the verification of the theory to the experiments, the theory is applied to the

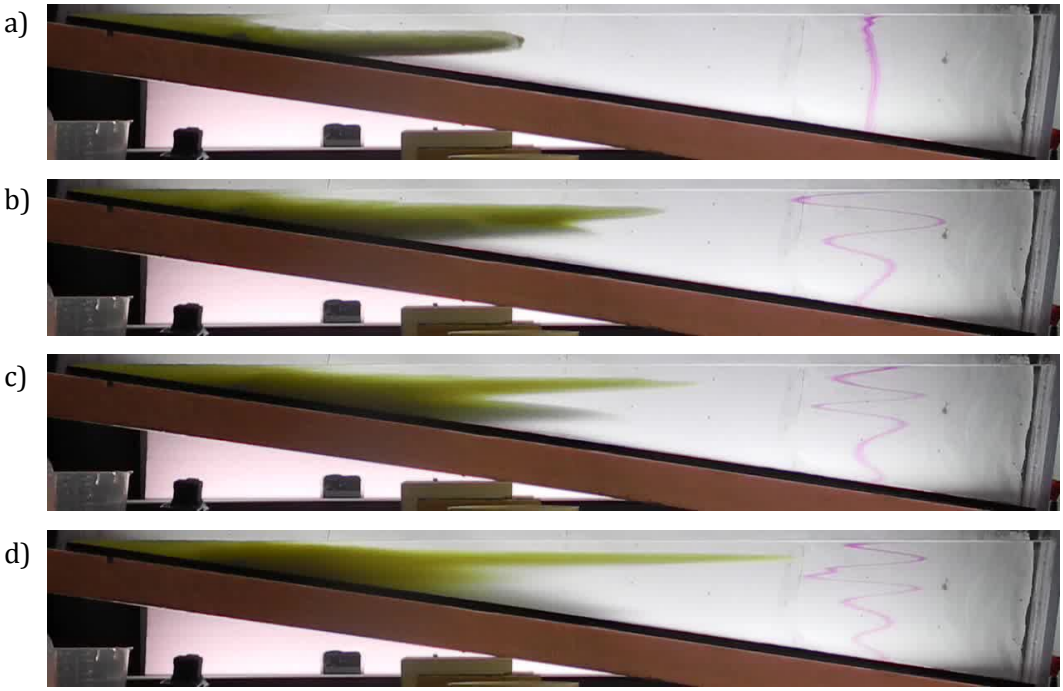

Figure 11: Flow of a particle laden current in constant density ambient of density 1.07 g cm^{-3}, $\rho_0 = 1.18$ g cm^{-3} with interstitial fluid density 0.998 g cm^{-3}, $d = 1 - 38$ μm and $h_0 = 3$ cm where a) the initial intrusion carries the particles within it until they slowly separate from the flow in b) and a distinct particle layer develops in c) slowly settling to the bottom at the settling velocity and carrying no more than marginal amounts of interstitial to lower depths d).

situation presented in [8], providing a means to determine the required particle concentration for a hyperpycnal plume to intrude at a certain depth. The results provide a more robust indication of the particle concentrations required to allow the flow to not return to the surface and indicate the simple applicability of the scaling theory to the real world. Further, the effect of the stratification to inhibit the presence of convective instabilities produced from the settling particles indicates the necessity to incorporate the key characteristics of both slope and stratification in order to more fully understand and represent the nature of particle laden currents. Hence, overall, by incorporating both these terms, the main effects influencing outflowing turbidity entering the ocean are represented and as such, a more complete picture of the nature of such flows is found.

7 Acknowledgement

I would like to thank Bruce Sutherland, whose guidance and input allowed my project to be possible and to progress as it did. I would also like to thank the organiser of the summer school for putting together such an amazing program and Paul Linden for teaching us so

much in those initial days. Thanks also go to George Veronis for giving his time to force us away from our work and inspiring us to have fun together and even, somehow, win a few softball games. And lastly of course I would like to thank the fellows for all the fun times and adventures we shared.

References

[1] P. G. Baines, *Mixing in downslope flows in the ocean Ð plumes versus gravity currents*, J. Fluid Mech., 443 (2001), pp. 237–270.

[2] ——, *Mixing in flows down gentle slopes into stratified environments*, Atmos.-Ocean, 46 (2008), pp. 405–419.

[3] T. B. Benjamin, *Gravity currents and related phenomena*, J. Fluid Mech., 31 (1968), pp. 209–248.

[4] R. T. Bonnecaze, H.E. Huppert, and J.R. Lister, *Particle-driven gravity currents*, J. Fluid Mech., 250 (1993), pp. 339–369.

[5] R. T. Bonnecaze and J. R. Lister, *Particle-driven gravity currents down planar slopes*, J. Fluid Mech., 390 (1999), pp. 75–91.

[6] S. F. Bradford, *Numerical Modelling of Turbidity Current Hydrodynamics and Sedimentation*, PhD thesis, University of Michigan, 1996.

[7] R. E. Britter and P. F. Linden, *The motion of the front of a gravity current travelling down an incline*, J. Fluid Mech., 99 (1980), pp. 531–543.

[8] G. K. C. Clark, A. B. G. Bush, and J. W. M. Bush, *Freshwater discharge, sediment transport, and modeled climate impacts of the final drainage of glacial lake agassiz*, J. Climate, 22 (2009), pp. 2161–2180.

[9] F. de. Rooij, *Sedimenting particle-laden flows in confined geometries*, PhD thesis, University of Cambridge, 1999.

[10] R. Fernandez and J. Imberger, *Time-varying underflow into a continuous stratification with bottom slope*, J. Hydraul. Eng., 134 (2008), pp. 1191–1198.

[11] M. Garcia and G. Parker, *Experiments on the entrainment of sediment into suspension by a dense bottom current*, J. Geophys. Res., 98 (1993), pp. 4793–4807.

[12] A. J. Hogg, H. E. Huppert, and M. A. Hallworth, *Reversing buoyancy of particle-driven gravity current*, Phys. Fluids, 11 (1999), pp. 2891–2900.

[13] ——, *Particle-driven gravity currents: asymptotic and box model solutions*, Eur. J. Mech. B Fluids, 19 (2000), pp. 139–165.

[14] H. E. Huppert, *Gravity currents: a personal perspective*, J. Fluid Mech., 554 (2006), pp. 299–322.

[15] B. E. Hurzeler, G. N. Ivey, and J. Imberger, *Spreading model for a turbidity current with reversing buoyancy from a constant-volume release*, Mar./ Freshwater/ Res., 46 (1995), pp. 393–408.

[16] B. Kneller and C. Buckee, *The structure and fluid mechanics of turbidity currents: a review of some recent studies and their geological implications*, Sedimentology, 47 (2000), pp. 62–94.

[17] A. A. Lawrence, W. D. McCaffrey, and P. J. Talling, *Special issue introduction: Sediment gravity flows Ð recent insights into their dynamic and stratified/composite nature*, Marine and Petroleum Geology, 26 (2009), pp. 1897–1899.

[18] D. G. Masson, R. G. Arzola, R. B. Wynn, J. E. Hunt, and P. P. E. Weaver, *Seismic triggering of landslides and turbidity currents offshore portugal*, Geochemistry, Geophysics, Geosystems, 12 (2011).

[19] T. Maxworthy, J. Leilich, J. E. Simpson, and E. H. Meiburg, *The propagation of a gravity current into a linearly stratified fluid*, J. Fluid Mech., 453 (2002), pp. 371–394.

[20] E. Meiburg and B. Kneller, *Turbidity currents and their deposits*, Annu. Rev. Fluid Mech., 42 (2010), pp. 135–156.

[21] J. J. Monahgan, R. A. F. Cas, A. M. Kos, and M. Hallworth, *Gravity currents descending a ramp in a stratified tank*, J. Fluid Mech., 379 (1999), pp. 39–69.

[22] T. Mulder and J. P. M. Syvitski, *Gravity currents descending a ramp in a stratified tank*, Journal of Geology, 103 (1995), pp. 285–299.

[23] T. Mulder, J. P. M. Syvitski, S. Migeon, J. C. Faugeres, and B. Savoye, *Marine hyperpycnal flows: initial, behaviour and related deposits. a review*, Marine and Petroleum Geology, 20 (2003), pp. 861–882.

[24] G. Parker, Y. Fukushima, and H. M. Pantin, *Self accelerating turbidity currents*, J. Fluid Mech., 171 (1986), pp. 145–181.

[25] J. P. Parson, J. W. M. Bush, and J. P. M. Syvitski, *Hyperpycnal plume formation from riverine outflows with small sediment concentration*, Sedimentology, 48 (2001), pp. 465–478.

[26] C. K. Paull, W. Ussler III, H. G. Greene, R. Keaten, P. Mitts, and J. Barry, *Caught in the act: the 20 december 2001 gravity flow event in monterey canyon*, Geo-Mar Lett, 22 (2003), pp. 227–232.

[27] C. Primez and J. Irman, *Reconstruction of turbidity currents in amazon channel*, Marine and Petroleum Geology, 20 (2003), pp. 823–849.

[28] F. P. Shepard, P. A. McLoughlin, N. F. Marshall, and G. G. Sullivan, *Current-meter recordings of low-speed turbidity currents*, Geology, 5 (2013), pp. 297–301.

[29] J. O. Shin, S. B. Dalziel, and P. F. Linden, *Gravity currents produced by lock exchange*, J. Fluid Mech., 521 (2004), pp. 1–34.

[30] R. S. J. Sparks, R. T. Bonnecaze, H. E. Huppert, J. R. Lister, M. A. Hallworth, H. Mader, and J. Phillips, *Sediment-laden gravity currents with reversing buoyancy*, Earth and Planetary Science Letters, 114 (1993), pp. 243–257.

[31] D. A. V. Stow, *Deep sea processes of sediment transport and deposition*, in Sediment Transport and Depositional Processes, K. Pye, ed., Blackwell Scientific Publications, Oxford, Boston, 1994, pp. 257–293.

[32] K. M. Straub, *Quantifying Turbidity Current Interaction with Topogrpahy*, PhD thesis, Massachusetts Institute of Technology, 2007.

[33] M. Ungarish, *On gravity currents in a linearly stratified ambient: a generalization of benjamin's steady-state propagation results*, J. Fluid Mech., 548 (2006), pp. 49–68.

[34] M. Wells and P. Nadarajah, *The intrusion depth of density currents flowing into stratified water bodies*, J. Phys. Oceanogr., 39 (2009), pp. 1935–1947.